NMRlipids IV: Headgroup & glycerol backbone structures, and cation binding in bilayers with PE and PG lipids

O. H. Samuli Ollila[1, 2, *]

[1] *Institute of Organic Chemistry and Biochemistry, Academy of Sciences of the Czech Republic, Prague 6, Czech Republic*
[2] *Institute of Biotechnology, University of Helsinki*

(Dated: October 22, 2019)

Primarily measured but also simulated NMR order parameters will be collected also for other than phophatidylcholine (these are discussed in NMRlipids I) headgroup. The information will be used to understand structural differences between different lipid molecules in bilayers.

INTRODUCTION

Zwitterionic PE is the second most abundant glycerophospholipid in eukaryotic cells and has been related to the diseases [**?** **?**]. PE and PG affect membrane protein functionality [**?**] and bind to various proteins [**?**].

In NMRlipids I and II project we were looking for a MD model which would correctly reproduce headgroup and glycerol backbone structures and cation binding for PC lipid bilayers [1, 2]. Here we extend the same goal for other than PC lipids. Currently the focus is on PE, PG and PS bilayers and their mixtures with PC. Experimental data with different amounts of added salt is now collected and presented in this manuscript.

Experimental order parameters for different lipid headgroups are collected in Fig. 1.

Based on superficial reading, the conclusions in the literature are roughly
1) glycerol backbone structures are largely similar irrespectively of the headroup [3],
2) glycerol backbone and headgroup structure and behaviour are similar in model membranes and in bacteria [3–5],
3) headgroup structures are similar in PC, PE and PG lipids, while headgroup is more rigid in PS lipids [6, 7].
Extensive discussion about structural details of PE, PG or PS headgroups do not exists (as far as I know), In contrast to PC lipids (see [1] and references therein).

Several simulations containing PE, PG and PS lipids have been published [**?**], **1.List should be completed** however, glycerol backbone and headgroup order parameters are not compared to the experiments (based on superficial reading of literature).

METHODS

Experimental C–H bond order parameters

The headgroup and glycerol backbone C–H bond order parameter magnitudes and signs of POPE and POPG were determined by measuring the chemical-shift resolved dipolar splittings with a R-type Proton Detected Local Field (R-PDLF) experiment [8] and S-DROSS experiments [9] using natural abundance ^{13}C solid state NMR spectroscopy as described previously [10**?** , 11]. **2.The rest of the details to be written. I am not sure how much we need to repeat the NMRlipidsIVps paper.**

Molecular dynamics simulations

Molecular dynamics simulation data were collected using the Open Collaboration method [1], with the NMRlipids Project blog (`nmrlipids.blogspot.fi`) and GitHub repository (`github.com/NMRlipids/NMRlipidsIVotherHGs`) as the communication platforms. The simulated systems are listed in Tables I (pure PE and PG bilayers without additional ions). and III (mixtures and systems with additional ions). Further simulation details are given in the SI, and the simulation data are indexed in a searchable database available at `www.nmrlipids.fi`, and in the NMRlipids/MATCH repository (`github.com/NMRlipids/MATCH`).

The C–H bond order parameters were calculated directly from the carbon and hydrogen positions using the definition

$$S_{\mathrm{CH}} = \frac{1}{2}\langle 3\cos^2\theta - 1\rangle, \qquad (1)$$

where θ is the angle between the C–H bond and the membrane normal (taken to align with z, with bilayer periodicity in the xy-plane). Angular brackets denote average over all sampled configurations. The order parameters were first calculated averaging over time separately for each lipid in the system. The average and the standard error of the mean were then calculated over different lipids. Python programs that use the MDAnalysis library [12, 13] used for all atom simulations is available in Ref. 14 (`scripts/calcOrderParameters.py`). For united atom simulations, the trajectories with hydrogens having ideal geometry were constructed first using either buildH program [**?**] or (`scratch/opAAUA_prod.py`) in Ref. 14, and the order parameters were then calculated from these trajectories. This approach has been tested against trajectories with explicit hydrogens and the deviations in order parameters are small [**?** **?**]. The ion number density profiles were calculated using the `gmx density` tool of the Gromacs sofware package [15].

TABLE I: List of MD simulations with PE lipids.

lipid/counter-ions	force field for lipids / ions	NaCl (M)	[a]N_l	[b]N_w	[c]N_c	[d]T (K)	[e]t_{sim}(ns)	[f]t_{anal} (ns)	[g]files
POPE	CHARMM36 [**?**]	0	144	5760	0	310	500	400	[16]
POPE	CHARMM36 [**?**]	0	500	25000	0	310	500	100	[17]
POPE	CHARMM36 [**?**]	0.11	500	25000	50	310	500	100	[18]
POPE	CHARMM36ua [**?**]	0	336	15254	0	310	2×200	2×100	[19]
DPPE	Slipids [20]	0	288	9386	0	336	200	100	[21]
POPE	Slipids [20**?**]	0	336	?	0	310	2×200	2×100	[22]
POPE	Slipids [**?**]	0	500	25000	0	310	500	100	[23]
POPE	Slipids [**?**] 3.	0.11	500	25000	50	310	500	100	[24]
DPPE	GROMOS-CKP [**?**]	0	128	3655	0	342	2×500	2×400	[25]
POPE	GROMOS-CKP [**?**]	0	128	3552	0	313	2×500	2×400	[26]
POPE	GROMOS-CKP [**?**]	0	500	25000	0	310	500	100	[27]
POPE	GROMOS-CKP [**?**]	0.11	500	25000	50	310	500	100	[28]
DOPE	GROMOS-CKP [**?**]	0	128	4789	0	271	2×500	2×400	[29]
POPE	GROMOS 43A1-S3 [**?**]	0	128	3552	0	313	2×200	2×100	[30]
POPE	OPLS-UA vdW on H [**?**]	0	128	3328	0	303	2×200	2×100	[31]
POPE	OPLS-UA [**?**]	0	128	3328	0	303	2×200	2×100	[32]
POPE	Berger-Vries [**?**]	0	128	3552	0	303	2×200	2×100	[33]
POPE	Berger-largeH [**?**]	0	128	3552	0	303	2×200	2×100	[34]
DOPE	Berger-Vries [**?**]	0	128	4789	0	271	2×200	2×100	[35]
DOPE	Berger-largeH [**?**]	0	128	4789	0	271	2×300	2×100	[36]
POPE	LIPID17 [**?**]	0	500	25000	50	310	500	100	[37]
POPE	LIPID17 [**?**]	0.11	500	25000	50	310	500	100	[38]

[a]Number of lipid molecules with largest mole fraction
[b]Number of water molecules
[c]Number of additional cations
[d]Simulation temperature
[e]Total simulation time
[f]Time used for analysis
[g]Reference for simulation files

TABLE II: List of MD simulations with PG lipids.

lipid/counter-ions	force field for lipids / ions	NaCl (M)	[a]N_l	[b]N_w	[c]N_c	[d]T (K)	[e]t_{sim}(ns)	[f]t_{anal} (ns)	[g]files
POPG/K^+	CHARMM36 [**?**] 4.	0	118	4110	0	298	100	100	[39]
POPG	CHARMM36 [**?**]	0.11	500	25000	49	310	500	100	[40]
POPG	CHARMM36 [**?**]	0	500	25000	0	310	500	100	[41]
POPG/Na^+	Slipids [42]	0	288	10664	0	298	250	100	[43]
DPPG/Na^+	Slipids [42]	0	288	11232	0	314	200	100	[44]
DPPG/Na^+	Slipids [42]	0	288	11232	0	298	400	100	[45]
POPG	Slipids [**?**] 5.	0	500	25000	0	310	500	100	[46]
POPG	Slipids [**?**] 6.	0.11	500	25000	49	310	500	100	[47]
POPG	LIPID17 [**?**]	0	500	25000	0	310	500	100	[48]
POPG	LIPID17 [**?**]	0.11	500	25000	49	310	500	100	[49]
POPG	GROMOS-CKP [**?**]	0	500	25000	0	310	500	100	[50]
POPG	GROMOS-CKP [**?**]	0.11	500	25000	49	310	500	100	[51]

[a]Number of lipid molecules with largest mole fraction
[b]Number of water molecules
[c]Number of additional cations
[d]Simulation temperature
[e]Total simulation time
[f]Time used for analysis
[g]Reference for simulation files

TABLE III: List of MD simulations with PE and PG lipids mixed with PC.

lipid/counter-ions	force field for lipids / ions	NaCl (M)	$CaCl_2$ (M)	[a]N_l	[b]N_w	[c]N_c	[d]T (K)	[e]t_{sim}(ns)	[f]t_{anal} (ns)	[g]files
POPC	CHARMM36 [**?**]	0.11	0	500	25000	48	310	500	100	[52]
POPC:POPG (7:3)	CHARMM36 [**?**]	0.11	0	350	?	?	310	500	100	[53]
POPC:POPG (1:1)/K^+	CHARMM36 [**?**]	0	0	250:250	18158	0	298	200	200	[54]
POPC:POPG (1:1)	CHARMM36 [**?**]	0	0.34 7.	250:250	20798	128	298	200	200	[55]
POPC:POPG (1:1)	CHARMM36 [**?**]	0	1.36 8.	250:250	18114	445	298	200	200	[56]
POPC:POPG (4:1)/K^+	CHARMM36 [**?**]	0	0	400:100	18664	0	298	200	200	[57]
POPC:POPG (4:1)/K^+	CHARMM36 [**?**]	0	1.0 9.	400:100	18647	419	298	200	200	[58]
POPC	CHARMM36 [**?**]	0	0	256	8704	0	300	300	250	[59]
POPC:POPE (1:1)	CHARMM36 [**?**]	0	0	128	8704	0	300	300	250	[60]
POPC	Slipid [**?**]	0.11	0	500	25000	48	310	500	100	[61]
POPC:POPG (7:3)	Slipid [**?**]	?	0	?	?	?	310	500	100	[**?**] 10.
POPC	Berger [**?**] 11.	0	0	256	10240	0	300	300	200	[62]
POPC:POPE (1:1)	Berger [**?**] 12.	0	0	128	11008	0	300	300	200	[63]
POPC:DOPE (1:1)	Berger [**?**] 13.	0	0	128	10240	0	300	300	200	[64]
DOPC	Berger [**?**] 14.	0	0	256	11008	0	300	300	200	[65]
DOPC:DOPE (1:1)	Berger [**?**] 15.	0	0	128	11008	0	300	300	200	[66]

[a]Number of lipid molecules with largest mole fraction
[b]Number of water molecules
[c]Number of additional cations
[d]Simulation temperature
[e]Total simulation time
[f]Time used for analysis
[g]Reference for simulation files

16.Data for POPC:POPG mixtures by listed by Antonio Peon is missing from this table

RESULTS AND DISCUSSION

Headgroup and glycerol backbone order parameters of POPE and POPG from ^{13}C NMR

The glycerol backbone and α-carbon peaks in INEPT spectra of POPE were assigned based on previously measured POPC spectra (Fig. S1) [10]. The β-carbon peak was assigned based on ^{13}C chemical shift table for amines available at `https://www.chem.wisc.edu/areas/reich/nmr/c13-data/cdata.htm`. The order parameters for the glycerol backbone and headgroup C–H bonds were determined from 2D-RPDLF and S-DROSS experiments (Fig. S1), as described previously [**?**]. The POPE experiments were recorded at 310 K, where the bilayer is in liquid disordered phase [**?**]. **17.Details to be checked by Tiago.**

18.Figure and discussion about POPG experiments to be addded.

The headgroup and glycerol backbone order parameters of PE lipids are similar with different acyl chains and also close the values for POPC, althought PE gives systematically slightly more positive values (Fig. 1). These could be explained with slightly larger temperature in PE measurements, except for the α-carbon with the positive sign, for which the more positive value is farther away from zero. For PG lipids, the glycerol backbone order parameters are more positive than for other lipids. The headgroup α-carbon gives value close to PE, while the value of β-carbon is distinct from other lipid being only one which has positive sign, suggesting distinct conformation of PG lipids in this region. This was not observed in previous ^{2}H NMR study, where sign was not measured and β-carbon order parameter was apparently similar to the value for PE and PC results.

In conclusion, the results suggests that the glycerol backbone conformations in all lipids are relatively similar. Also, the headgroup conformations are similar for PC and PE lipids, while PS and PG are singnificantly different. For PS lipids, the differences are discussed previously [**?**].

Headgroup and glycerol backbone of POPE and POPG in MD simulations

As reported previously for PC [1] and PS [**?**] lipids, the headgroup and glycerol backbone order parameters show wide variation between different force fields for both PE and PG lipids (Figs. 2 and 3), and none of the force fields reproduce all values within experimental error bars. The poor performance of headgroup order parameters in Berger model can be probably explained by ring like structures seen in Fig. 6 in Ref. 70, which is a typical feature for Berger based lipid force fields containing explicit hydrogen atoms in the head group [71–73].

Also in line with previous studies for PC [1] and PS [**?**] lipids, CHARMM36 simulations are in best agreement with experiments for headgroup and glycerol backbone order parameters, and seem to capture all the essential differences be-

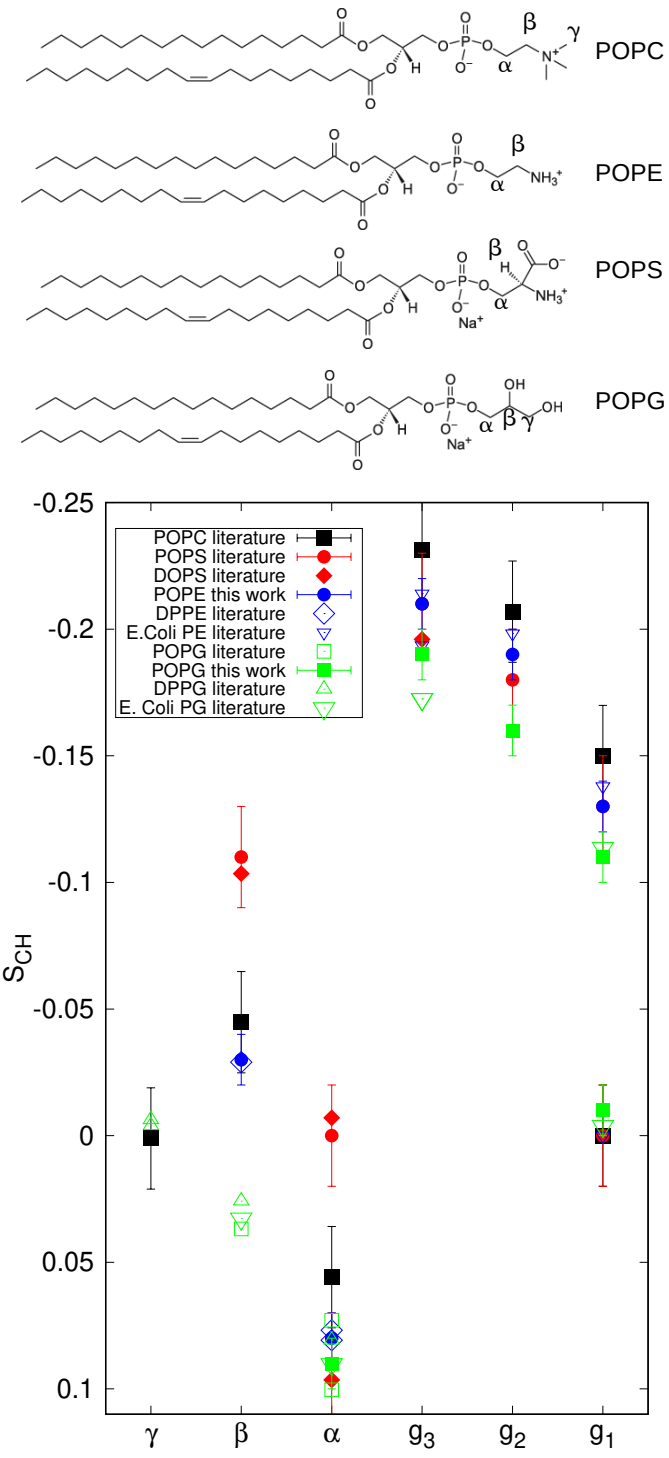

FIG. 1: (top) Chemical structure of different lipids (bottom) Headgroup and glycerol backbone order parameters measured from lipids with different headgroups in lamellar liquid disordered phase. The values and signs for POPE (310 K), POPG (298 K). POPS (298 K) [**?**] and POPC (300 K) [10, 11] are measured using ^{13}C NMR. The literature values for DOPS with 0.1M of NaCl (303 K) [67], POPG with 10nM PIPES (298 K) [68], DPPG with 10mM PIPES and 100mM NaCl (314 K) [6], DPPE (341 K) [69], E.coliPE and E.coliPG (310 K) [3] are measured using ^{2}H NMR. The signs from ^{13}C NMR are used also for the literature values.

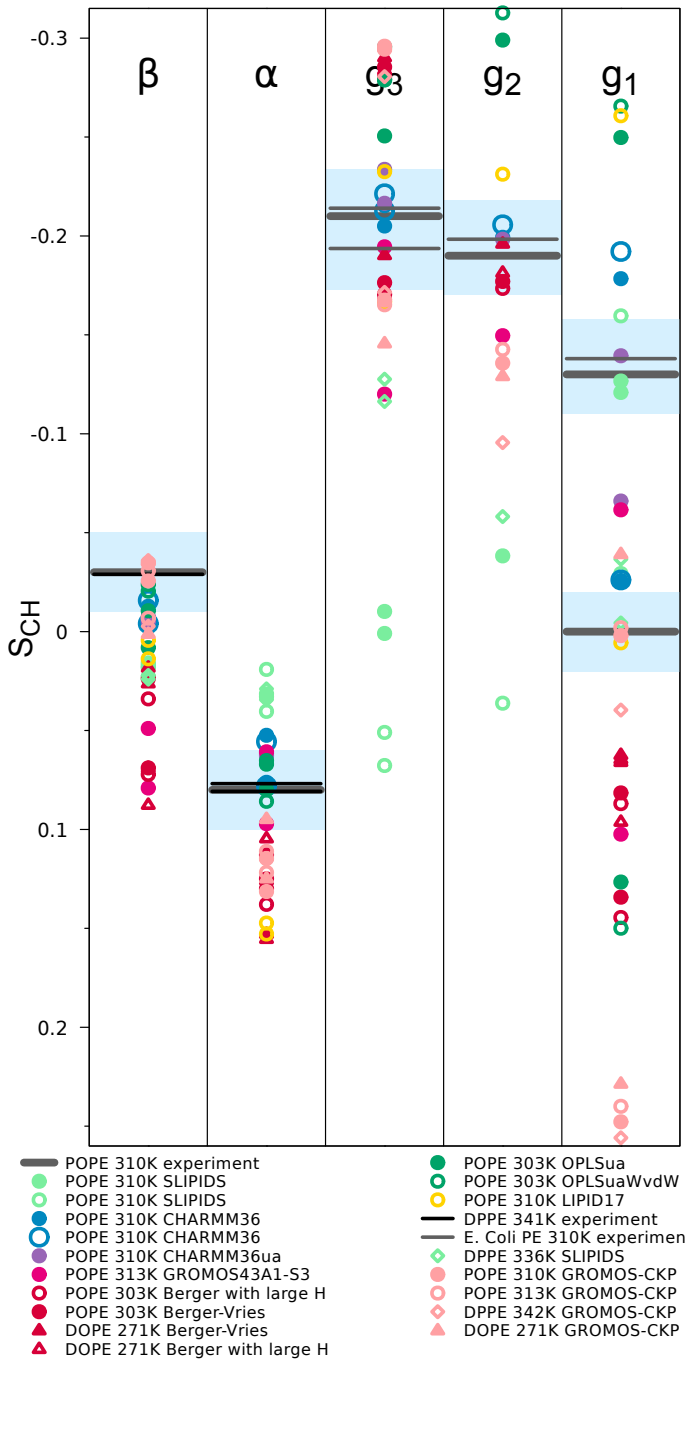

FIG. 2: The headgroup and glycerol backbone order parameters of PE lipids from experiments (POPE and signs this work, DPPE from Ref. 69 and E.coliPE from Ref. 3) and simulations with different force fields.

19.This should be clarified as in NMRlipidsI and error bars should be added. Probably larger error bars for united atom models based on the report by Fuchs et al.

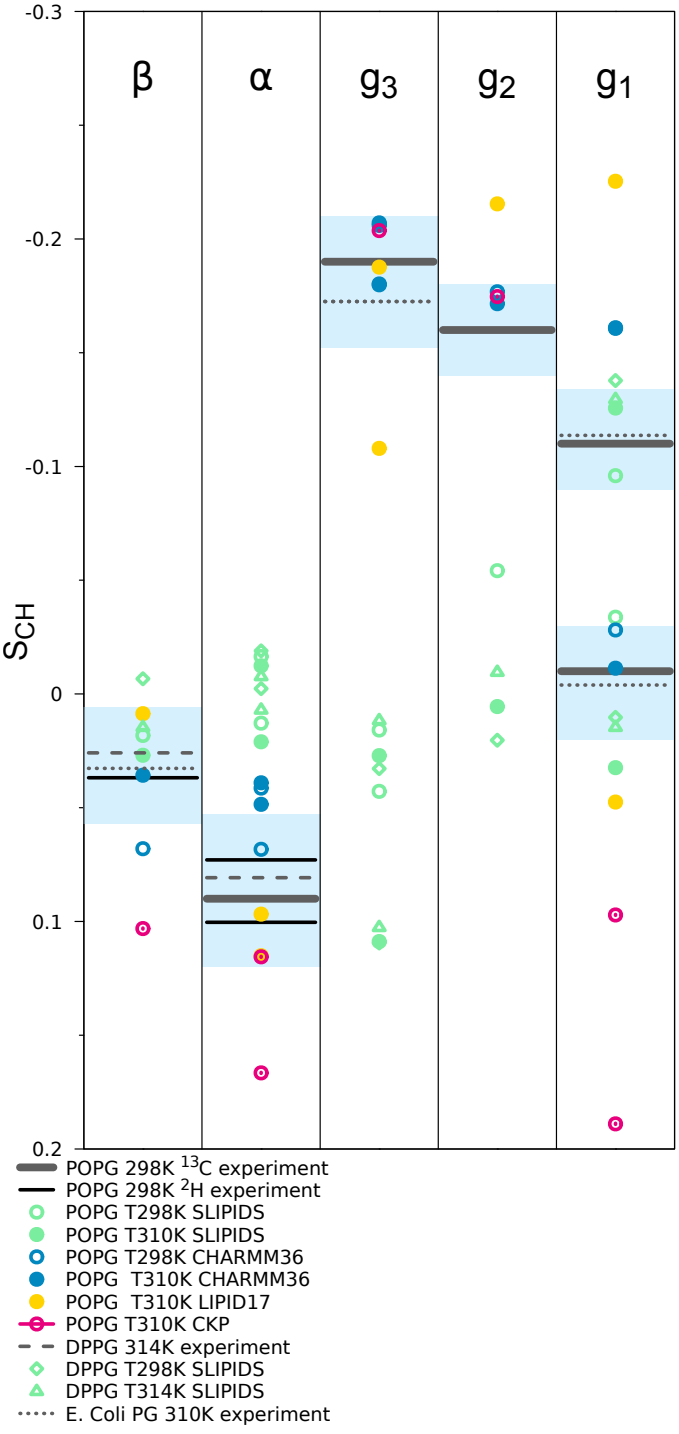

FIG. 3: The headgroup and glycerol backbone order parameters of PG lipids from experiments (POPG and signs from this work and from Ref. 68, DPPG with 100mM NaCl from Ref. 6,and E.Coli PG results from Ref. 3). and simulations with different force fields.

tween different headroups (Figs. 2 and 3). In previous study, CHARMM36 predicted the more negative β-carbon order parameter and larger forking of the α-carbon is PS headgroup than in PC [**?**]. In this work, the CHARMM36 simulations

reproduce also the other essential differences in experimental headgroup order parameters between different headgroups (Fig. 1) despite the inaccuracies in individual segments: The PE headgroup order parameters in CHARMM36 simulations are similar to the PC [1] and β-carbon order parameters is positive in PG headgroup, in contrast to the negative values observed in other lipids. Therefore, we use CHARMM36 simulations to analyze the structural differences between headgroups (Fig. 4). While rotation around N-C_α-C_β-O_α dihedral was significantly different in PS and PC headgroups in previous work [**?**], essential differences between PC, PE and PG are not observed here (Fig. 4) **20.We need also the dihedral distributions to finish this discussion..**

21.Why is the β-carbon order parameter of PG different to PC and PE then?

PC headgroup interactions with PE and PG

According to the electrometer concept, the PC headgroup order parameters increase with the addition of negatively charged PG or PS lipids, but are not affected by the addition of zwitterionic PE and SM lipids or cholesterol (Fig. 5) [4, 76, 77]. The different responses of PC headgroup order parameters to PE and PG are roughly reproduced in CHARMM36 simulations, although the changes are slightly overestimated upon addition of PE and underestimated upon addition of PG (Fig. 5). Interestingly, the response of POPC headgroup order parameters to POPE is close to experiments also in Berger-OPLS simulations, even though the response of Berger force field to cholesterol was significantly overestimated in our previous work [1]. In all force fields except Slipids, the α-carbon order parameters of different hydrogens are responsing differently when mixed with PE or PG lipids **23.Maybe we should figure out what is the reason for this. 24.Maybe we should analyze the P-N vector angle from different simulations.**

For β-carbon order parameter in PG headgroup, experiments report mild increase [74] or no change [68] upon addition of PC lipids (Fig. 6). Simulations with all the tested force fields give only very small changes also for the α-carbon order parameter (Figs. S2 and 6). Therefore, the simulations are generally in line with experimetns, suggesting that the interactions with PC do not essentially effect the PG headgroup structure. This is in contrast with previous results for PS headgroup [77], where all the force fieds significantly overestimated the structural response of PS headgroup to the interactions with PC lipids.

25.This is text by P. Fuchs, copied from the blog.

Area results in nm^2, the error is $<=$ 0.003 nm^2

- pure POPC

CHARMM36: 0.624

Berger : 0.649

- POPC/POPE 50:50

CHARMM36 : POPC 0.609, POPE 0.557

Berger-hacked: POPC 0.637, POPE 0.632

—

One can see that CHARMM 36 predicts a drop in the area on going from pure POPC to POPC/POPE 50:50. This means that POPC pack tightly to POPE. In contrast, the values for Berger are not that changed. The POPE value predicted by CHARMM 36 (in the mixture POPC/POPE 50:50) is much smaller than that predicted by Berger.

——-

The experimental acyl chain order parameters for POPE [78] seem larger than reported for POPC [10], which supports the more condensed PE bilayer. This is interesting, but to avoid the overexapansion of the manuscript, it is probably better to keep the focus in headgroups and ion binding also in this manuscript.

Sodium binding to PE and PG lipid bilayers

In our previous study about PS lipids [77], the underestimated increase of PC headgroup order parameters upon addition of negaticely charged lipids was related to the overestimated counterion binding affinity, which would overcompensates the effect of negative charge. Similar correlation is observed here in Lipid 17 simulations, which exhibits stronger counter-ion binding affinity to pure POPG bilayer (Fig. 7) and larger decrease in POPC β carbon order parameter upon addition of POPG than other simulations. Together with the lower area per molecule (59.5 Å^2) than in experiments (66.1 Å^2), the results suggest that the counterions bind too strongly and shield the electrostatic repulsion between PG headgroups in bilayers simulated with Lipid17 parameters. In GROMOS-CKP simulations, however, the β-carbon order parameter of POPC increases upon addition of POPG more than in CHARMM36 and Slipids simulations even though the binding affinities in these simulations are similar. On the other hand, the responses of different hydrogens attached in α-carbons are different in all simulations except in Slipids, most sever in Lipid17 and GROMOS-CKP where other in increases and other decreases **26.Can we figure out the reason for this?**. In conclusion, the counter-ion binding seems to be overestimated in Lipid17 with the strongest affinity among the tested models, while with this data we cannot fully evaluate binding affinity in the other models.

Similarly to POPG, the Lipid17 exhibits stronger sodium binding affinity to POPE bilayers than Slipids, CHARMM36 and GROMOS-CKP (Fig. 8). In Lipid17 the sodium binding affinity to POPE is approximately similar as to POPC, while in other models exhibit weaker binding to POPE (Fig. S3). The difference is small in Slipids and CHARMM36, while GROMOS-CKP predicts subtantially stronger binding to POPC. Experimental data for sodium binding to PE lipids is not available, while simulations in agreement with electrometer data from NMR suggests that sodium binding to POPC is weaker than in any of the simulations here (Fig. S3) [2, 80]. Assuming that the binding to POPE would be similar than to POPC, the sodium binding affinity to POPE is potentially realistic in CHARMM36, Slipids, and GROMOS-CKP simulations here, but substantially overestimated in Lipid17 simulation. **27.The potential differences in the used ion models should be checked.**

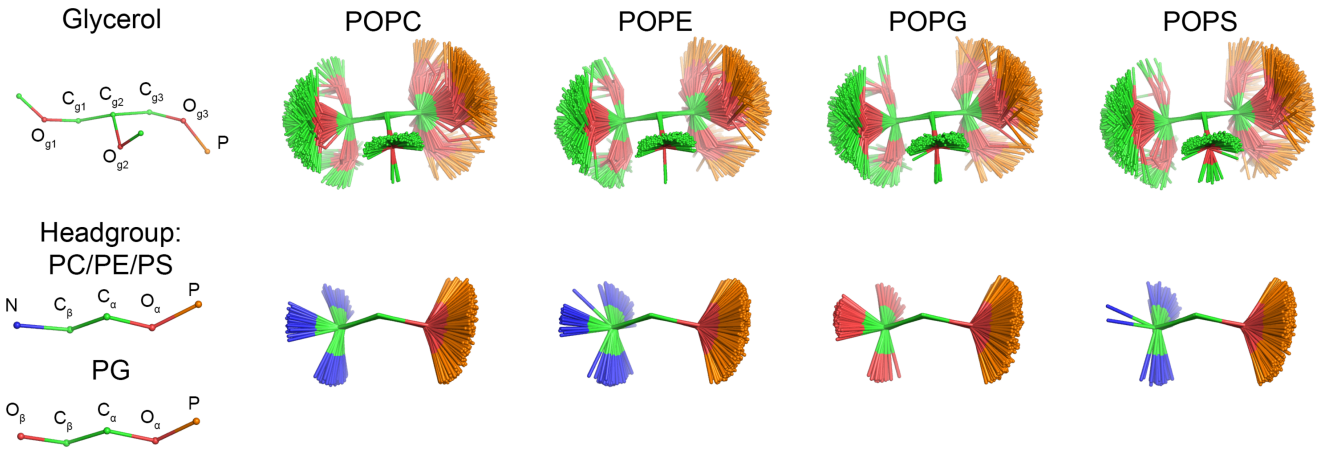

FIG. 4: Overlayed snapshots from CHARMM36 simulations of different lipids which give the best agreement with experiments.

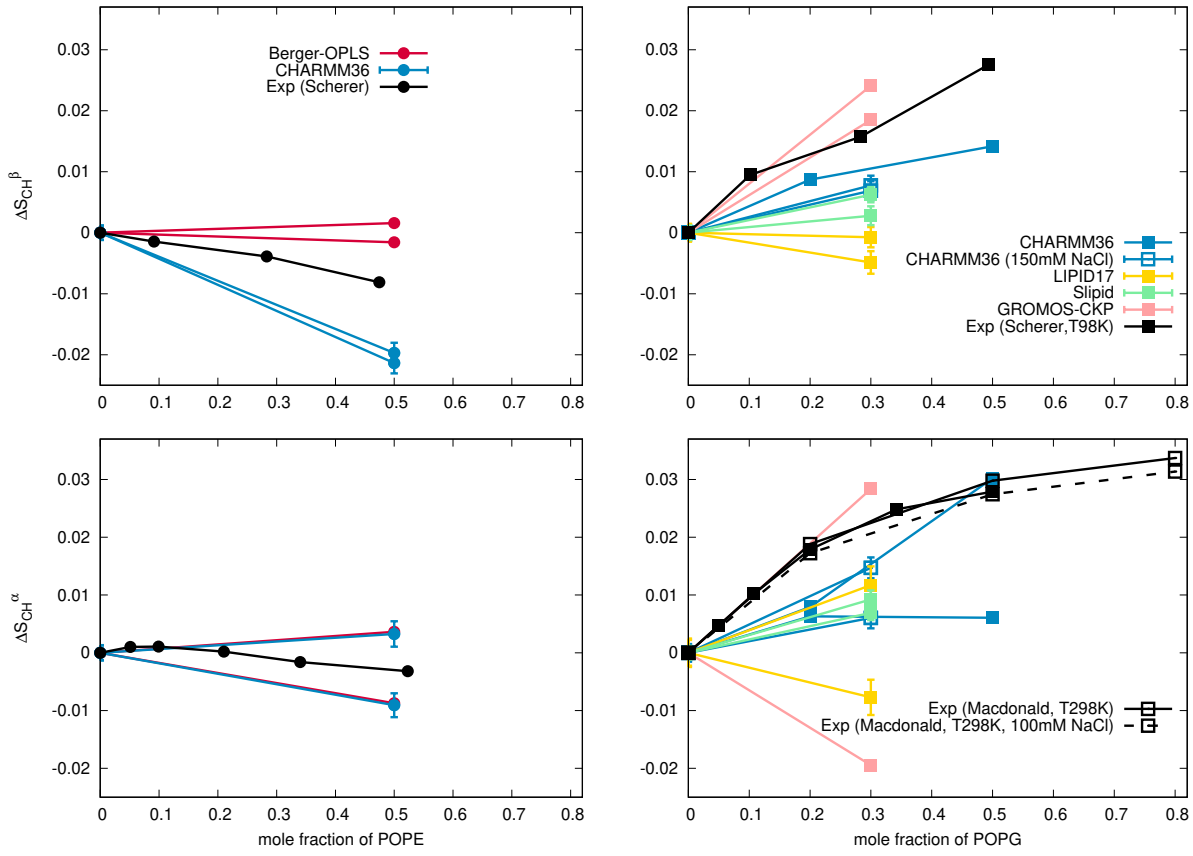

FIG. 5: Modulation of POPC headgroup order parameters with increasing amount of POPE (left) and POPG (right) in bilayer from experiments [4, 74] and simulations with different force fields. Signs are determined as discussed in [1, 75].

22.Data for CHARMM without ions to be added once this issue is solved: https://github.com/NMRLipids/MATCH/issues/83

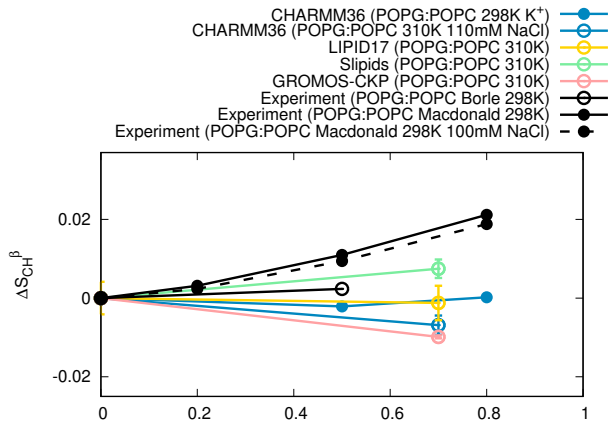

FIG. 6: Modulation of PG lipid headgroup order parameters with the increasing amount of PC in lipid bilayer from experiments [68, 74] and simulations with different force fields.

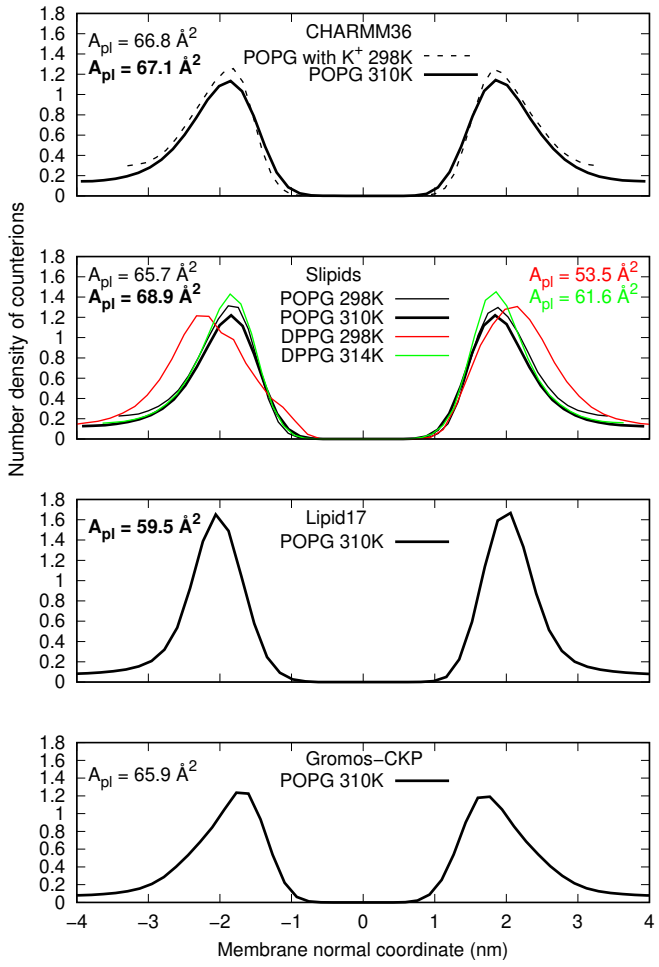

FIG. 7: Counterion densities and area per lipids from simulations with PG lipids. Experimental area for POPG at 303 K is 66.1 Å^2 and 67 Å^2 for DPPC at 323 K [79].

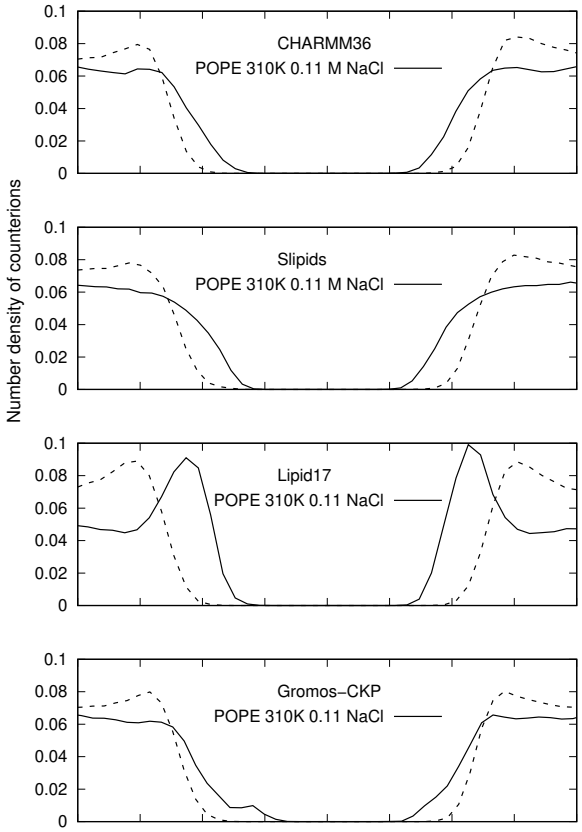

FIG. 8: Sodium (solid line) and choride ion density profiles along membrane normal from different simulations with PE lipids.

Cation binding to PE and PG lipid bilayers

The headgroup order parameters of PC lipids can used to measure ion binding affinity to lipid bilayers, because their magnitude is linearly proportional to the amount of bound charge in bilayer according to the molecular electrometer concept [2, 76]. The molecular electrometer concept can be used also for bilayers containing PC lipids mixed with charged lipids [68, 74, 81**?**]. Based on the electrometer concept and other data is has been suggested that [5]

> *"(i) Ca^{2+} binds to neutral lipids (phosphatidylcholine, phosphatidylethanolamine) and negatively charged lipids (phosphatidylglycerol) with approximately the same binding constant of K = 10-20 M^{-1};*
> *(ii) the free Ca^{2+} concentration at the membrane interface is distinctly enhanced if the membrane carries a negative surface charge, either due to protein or to lipid;*
> *(iii) increased inter-facial Ca^{2+} also means increased amounts of bound Ca^{2+} at neutral and charged lipids;*
> *(iv) the actual binding step can be described by a Langmuir adsorption isotherm with a 1 lipid:1 Ca^{2+} stoichiometry, provided the interfacial concentration C_M, is used to describe the chemical binding equilibrium."*

The electrometer concept has been very useful in evaluating ion binding affinity in simulations against experiments, because the headgroup order parameter changes as a function of ion concentration can be directly compared with experiments [2, 80**?**].

Calcium binding affinity to PC and PS lipid bilayers was not correctly described by any of the standard MD simulation forced fields [2**?**], while recently introduced force field with electronic continuum correction (ECC) performed better [80]. The decrease of α-carbon order parameter of PC lipids in PC:PG mixtures as a function of calcium concentration is close to experiments CHARMM36 simulations (Fig. 9), but the decrease of β-carbon order parameter seems to be overestimated. However, the β-carbon order parameter was not actually measured from these samples, but they are calculated from empirical relation $\Delta S_\beta = 0.43 \Delta S_\alpha$ [82]. The result is similar to the $\sim$200 ns simulations with PC lipids in previous work [2]. However, when simulation was continued for μs, the binding affinity substantially increased and interpretation was that calcium overbinds to PC lipid in CHARMM36. Therefore, the conclusion seems to be similar here, although the new NBfix parameters may complicate the situation **28.The status of NBfix parameters in these simulations should be checked.**.

The β-carbon order parameter of PG exhibits a rapid decrease with small $CaCl_2$ concentrations and a more modest decrease with larger concentrations in experiments [68] (Fig. **??**). The rapid decrease with $CaCl_2$ is observed but overestimated in CHARMM36 simulation with POPC:POPG 1:1 mixture, but not in 4:1 mixture **29.This is little bit weird, should be checked.**.

30.We need PC:PG simulations with $CaCl_2$ from different force fields to finish the discussion.

CONCLUSIONS

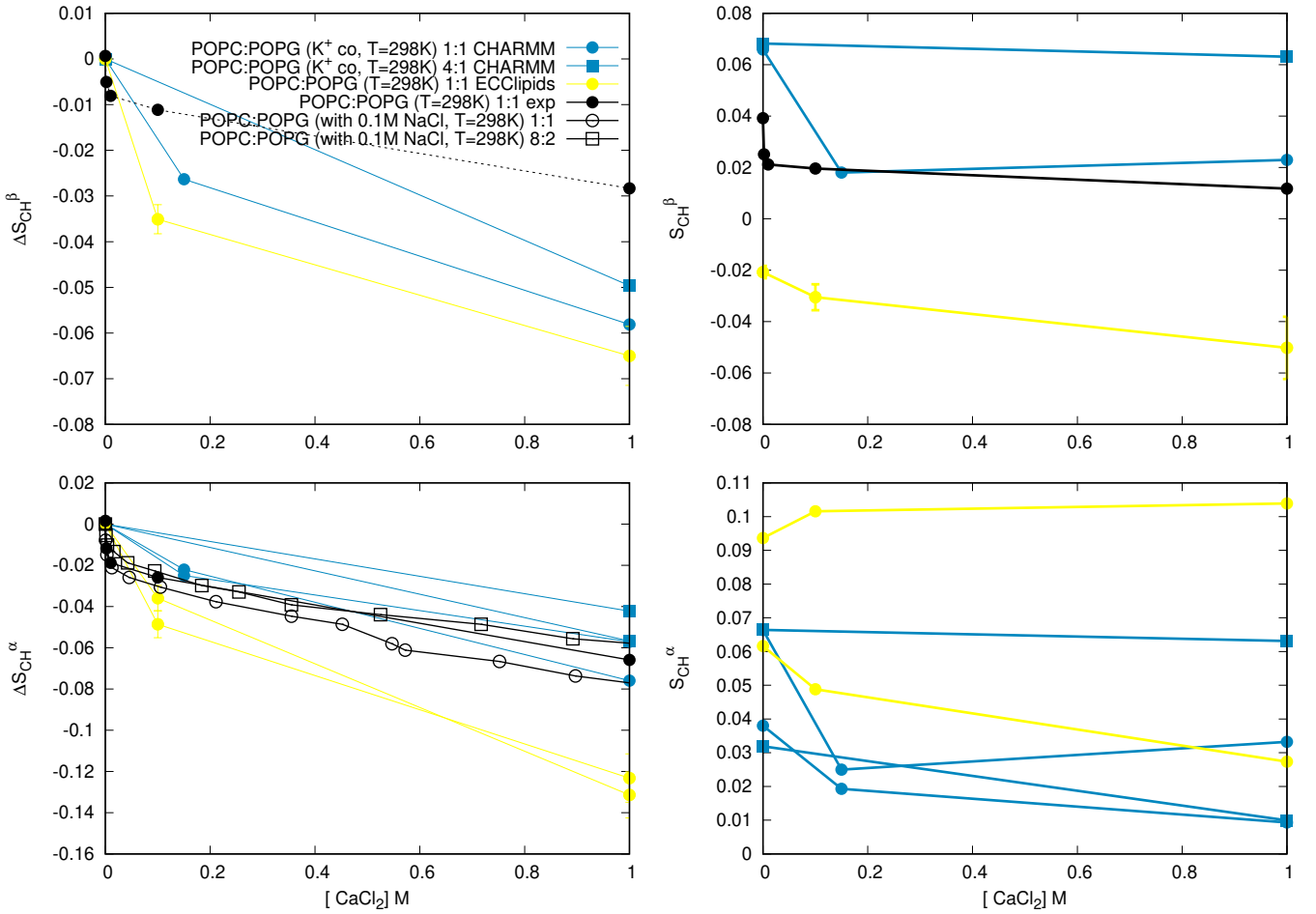

FIG. 9: (left) The headgroup order parameters of PC from PC:PG mixtures as a function $CaCl_2$ concentration from experiments [68, 74] and CHARMM36 simulations. Note that beta order parameter is calculated from empirical relation $\Delta S_\beta = 0.43\Delta S_\alpha$ [82], not actually measured. (right) The headgroup order parameters of PG from PC:PG mixtures as a function $CaCl_2$ concentration from experiments [68] and CHARMM36 simulations.

SUPPLEMENTARY INFORMATION

* samuli.ollila@helsinki.fi

[1] A. Botan, F. Favela-Rosales, P. F. J. Fuchs, M. Javanainen, M. Kanduč, W. Kulig, A. Lamberg, C. Loison, A. Lyubartsev, M. S. Miettinen, et al., J. Phys. Chem. B **119**, 15075 (2015).

[2] A. Catte, M. Girych, M. Javanainen, C. Loison, J. Melcr, M. S. Miettinen, L. Monticelli, J. Maatta, V. S. Oganesyan, O. H. S. Ollila, et al., Phys. Chem. Chem. Phys. **18**, 32560 (2016).

[3] H. U. Gally, G. Pluschke, P. Overath, and J. Seelig, Biochemistry **20**, 1826 (1981).

[4] P. Scherer and J. Seelig, EMBO J. **6** (1987).

[5] J. Seelig, Cell Biology International Reports **14**, 353 (1990), ISSN 0309-1651, URL http://www.sciencedirect.com/science/article/pii/030916519091204H.

[6] R. Wohlgemuth, N. Waespe-Sarcevic, and J. Seelig, Biochemistry **19**, 3315 (1980).

[7] G. Büldt and R. Wohlgemuth, The Journal of Membrane Biology **58**, 81 (1981), ISSN 1432-1424, URL http://dx.doi.org/10.1007/BF01870972.

[8] S. V. Dvinskikh, H. Zimmermann, A. Maliniak, and D. Sandstrom, J. Magn. Reson. **168**, 194 (2004).

[9] J. D. Gross, D. E. Warschawski, and R. G. Griffin, J. Am. Chem. Soc. **119**, 796 (1997).

[10] T. M. Ferreira, F. Coreta-Gomes, O. H. S. Ollila, M. J. Moreno, W. L. C. Vaz, and D. Topgaard, Phys. Chem. Chem. Phys. **15**, 1976 (2013).

[11] T. M. Ferreira, R. Sood, R. Bärenwald, G. Carlström, D. Topgaard, K. Saalwächter, P. K. J. Kinnunen, and O. H. S. Ollila, Langmuir **32**, 6524 (2016).

[12] N. Michaud-Agrawal, E. J. Denning, T. B. Woolf, and O. Beckstein, Journal of Computational Chemistry **32**, 2319 (2011), https://onlinelibrary.wiley.com/doi/pdf/10.1002/jcc.21787, URL https://onlinelibrary.wiley.com/doi/abs/10.1002/jcc.21787.

[13] Richard J. Gowers, Max Linke, Jonathan Barnoud, Tyler J. E. Reddy, Manuel N. Melo, Sean L. Seyler, Jan Domański, David L. Dotson, Sébastien Buchoux, Ian M. Kenney, et al., in *Proceedings of the 15th Python in Science Conference*, edited

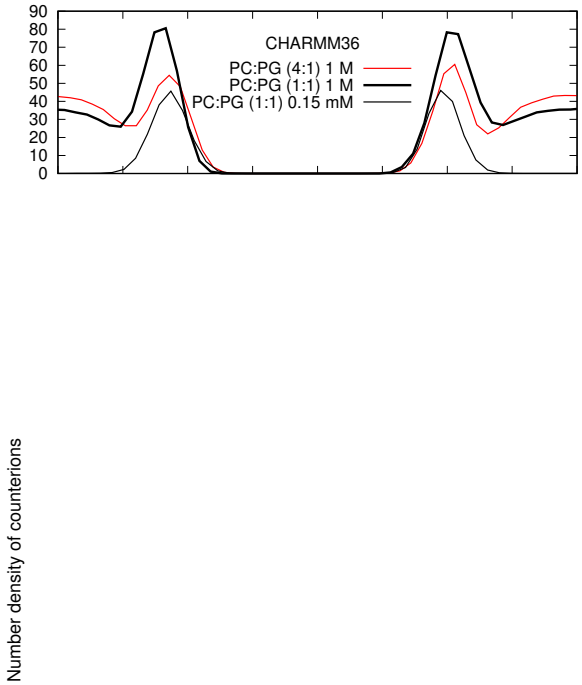

FIG. 10: Calcium ion density profiles along membrane normal from different simulations with PG lipids.

by Sebastian Benthall and Scott Rostrup (2016), pp. 98 – 105.

[14] ohsOllila and et al., *Match github repository*, URL https://github.com/NMRLipids/MATCH.

[15] M. Abraham, D. van der Spoel, E. Lindahl, B. Hess, and the GROMACS development team, *GROMACS user manual version 5.0.7* (2015), URL www.gromacs.org.

[16] M. Javanainen, *Simulation of a POPE bilayer at 310K with the CHARMM36 force field* (2019), URL https://doi.org/10.5281/zenodo.2641987.

[17] PEON, *CHARMM36 POPE Bilayer Simulation (Last 100 ns, 310 K)* (2019), URL https://doi.org/10.5281/zenodo.3237461.

[18] A. PEÓN, *CHARMM36 POPE Bilayer Simulation (Last 100 ns, 150 mM NaCl, 310 K)* (2019), URL https://doi.org/10.5281/zenodo.2577454.

[19] T. Piggot, *CHARMM36-UA POPE Simulations (versions 1 and 2) 310 K (NOTE: hexagonal membrane and POPE is called PEUA)* (2018), URL https://doi.org/10.5281/zenodo.1293774.

[20] J. P. M. Jämbeck and A. P. Lyubartsev, J. Chem. Theory Comput. **8**, 2938 (2012).

[21] F. Favela-Rosales, *MD simulation trajectory of a fully hydrated DPPE bilayer: SLIPIDS, Gromacs 5.0.4. 2017.* (2017), URL https://doi.org/10.5281/zenodo.495247.

[22] T. Piggot, *Slipids POPE Simulations (versions 1 and 2) 310 K (NOTE: hexagonal membrane)* (2018), URL https://doi.org/10.5281/zenodo.1293813.

[23] A. Peon, *SLIPID POPE Bilayer Simulation (Last 100 ns, 310 K)* (2019), URL https://doi.org/10.5281/zenodo.3231342.

[24] A. PEÓN, *SLIPID POPE Bilayer Simulation (Last 100 ns, 150 mM NaCl, 310 K)* (2019), URL https://doi.org/10.5281/zenodo.2578069.

[25] T. Piggot, *GROMOS-CKP DPPE Simulations (versions 1 and 2) 342 K* (2018), URL https://doi.org/10.5281/zenodo.1293957.

[26] T. Piggot, *GROMOS-CKP POPE Simulations (versions 1 and 2) 313 K* (2018), URL https://doi.org/10.5281/zenodo.1293932.

[27] A. PEON, *GROMOS POPE Bilayer Simulation (Last 100 ns, 310 K)* (2019), URL https://doi.org/10.5281/zenodo.3237754.

[28] A. PEÓN, *Gromos POPE Bilayer Simulation (Last 100 ns, 150 mM NaCl, 310 K)* (2019), URL https://doi.org/10.5281/zenodo.2574491.

[29] T. Piggot, *GROMOS-CKP DOPE Simulations (versions 1 and 2) 271 K* (2018), URL https://doi.org/10.5281/zenodo.1293941.

[30] T. Piggot, *GROMOS 43A1-S3 POPE Simulations (versions 1 and 2) 313 K (NOTE: anisotropic pressure coupling)* (2018), URL https://doi.org/10.5281/zenodo.1293762.

[31] T. Piggot, *OPLS-UA POPE Simulations (versions 1 and 2) 303 K with vdW on H atoms* (2018), URL https://doi.org/10.5281/zenodo.1293853.

[32] T. Piggot, *Opls-ua pope simulations (versions 1 and 2) 303 k* (2018), URL https://doi.org/10.5281/zenodo.1293855.

[33] T. Piggot, *Berger POPE Simulations (versions 1 and 2) 303 K - de Vries repulsive H* (2018), URL https://doi.org/10.5281/zenodo.1293889.

[34] T. Piggot, *Berger POPE Simulations (versions 1 and 2) 303 K - larger repulsive H* (2018), URL https://doi.org/10.5281/zenodo.1293891.

[35] T. Piggot, *Berger DOPE Simulations (versions 1 and 2) 271 K - de Vries repulsive H* (2018), URL https://doi.org/10.5281/zenodo.1293928.

[36] T. Piggot, *Berger DOPE Simulations (versions 1 and 2) 271 K - larger repulsive H* (2018), URL https://doi.org/10.5281/zenodo.1293905.

[37] A. PEON, *LIPID17 POPE Bilayer Simulation (Last 100 ns, 310 K)* (2019), URL https://doi.org/10.5281/zenodo.3378970.

[38] A. PEÓN, *LIPID17 POPE Bilayer Simulation (Last 100 ns, 150 mM NaCl, 310 K)* (2019), URL https://doi.org/10.5281/zenodo.2577305.

[39] O. H. S. Ollila, *POPG lipid bilayer simulation at T298K ran with MODEL_CHARMM_GUI force field and Gromacs* (2017), URL https://doi.org/10.5281/zenodo.1011096.

[40] A. PEÓN, *CHARMM36 POPG Bilayer Simulation (Last 100 ns, 150 mM NaCl, 310 K)* (2019), URL https://doi.

org/10.5281/zenodo.2573531.
[41] ANTONIO, *CHARMM36 POPG Bilayer Simulation (Last 100 ns, 310 K)* (2019), URL https://doi.org/10.5281/zenodo.3237463.
[42] J. P. M. Jämbeck and A. P. Lyubartsev, Phys. Chem. Chem. Phys. **15**, 4677 (2013).
[43] F. Favela-Rosales, *MD simulation trajectory of a fully hydrated POPG bilayer: SLIPIDS, Gromacs 5.0.4. 2017.* (2017), URL https://doi.org/10.5281/zenodo.546133.
[44] F. Favela-Rosales, *MD simulation trajectory of a fully hydrated DPPG bilayer @314K: SLIPIDS, Gromacs 5.0.4. 2017.* (2017), URL https://doi.org/10.5281/zenodo.546136.
[45] F. Favela-Rosales, *MD simulation trajectory of a fully hydrated DPPG bilayer @298K: SLIPIDS, Gromacs 5.0.4. 2017.* (2017), URL https://doi.org/10.5281/zenodo.546135.
[46] A. PEÓN, *SLIPID POPG Bilayer Simulation (Last 100 ns, 310 K)* (2019), URL https://doi.org/10.5281/zenodo.3364460.
[47] A. PEÓN, *SLIPID POPG Bilayer Simulation (Last 100 ns, 150 mM NaCl, 310 K)* (2019), URL https://doi.org/10.5281/zenodo.2633773.
[48] A. PEON, *LIPID17 POPG Bilayer Simulation (Last 100 ns, 310 K)* (2019), URL https://doi.org/10.5281/zenodo.3247659.
[49] A. PEÓN, *LIPID17 POPG Bilayer Simulation (Last 100 ns, 150 mM NaCl, 310 K)* (2019), URL https://doi.org/10.5281/zenodo.2573905.
[50] A. PEON, *GROMOS POPG Bilayer Simulation (Last 100 ns, 310 K)* (2019), URL https://doi.org/10.5281/zenodo.3266166.
[51] A. PEÓN, *Gromos POPG Bilayer Simulation (Last 100 ns, 150 mM NaCl, 310 K)* (2019), URL https://doi.org/10.5281/zenodo.3257649.
[52] A. Peón, *CHARMM36 POPC Bilayer Simulation (Last 100 ns, 150 mM NaCl, 310 K)* (2019), URL https://doi.org/10.5281/zenodo.2628335.
[53] A. PEÓN, *CHARMM36 POPC-POPG 7:3 Bilayer Simulation (Last 100 ns, 150 mM NaCl, 310 K)* (2019), URL https://doi.org/10.5281/zenodo.2580902.
[54] J. J. Madsen, *MD simulations of bilayers containing PC/PG mixtures and CaCl_2: 250POPC_250POPG_neutral* (2019), URL https://doi.org/10.5281/zenodo.3483787.
[55] J. J. Madsen, *MD simulations of bilayers containing PC/PG mixtures and CaCl_2: 250POPC_250POPG_0.15MCaCl_2* (2019), URL https://doi.org/10.5281/zenodo.3483789.
[56] J. J. Madsen, *MD simulations of bilayers containing PC/PG mixtures and CaCl_2: 250POPC_250POPG_1MCaCl_2* (2019), URL https://doi.org/10.5281/zenodo.3483793.
[57] J. J. Madsen, *MD simulations of bilayers containing PC/PG mixtures and CaCl_2: 400POPC_100POPG_neutral* (2019), URL https://doi.org/10.5281/zenodo.3483783.
[58] J. J. Madsen, *MD simulations of bilayers containing PC/PG mixtures and CaCl_2: 400POPC_100POPG_1MCaCl_2* (2019), URL https://doi.org/10.5281/zenodo.3483785.
[59] C. Papadopoulos and P. F. Fuchs, *CHARMM36 pure POPC MD simulation (300 K - 300ns - 1 bar)* (2018), URL https://doi.org/10.5281/zenodo.1306800.
[60] C. Papadopoulos and P. F. Fuchs, *CHARMM36 POPC/POPE (50%-50%) MD simulation (300 K - 300ns - 1 bar)* (2018), URL https://doi.org/10.5281/zenodo.1306821.
[61] A. PEÓN, *SLIPID POPC Bilayer Simulation (Last 100 ns, 150 mM NaCl, 310 K)* (2019), URL https://doi.org/10.5281/zenodo.2574689.
[62] B. Amélie and F. P. F.J., *Berger pure POPC MD simulation (300 K - 300ns - 1 bar)* (2018), URL https://doi.org/10.5281/zenodo.1402417.
[63] B. Amélie and F. P. F.J., *Berger POPC/POPE (50:50 ratio) MD simulation (300 K - 400ns - 1 bar)* (2018), URL https://doi.org/10.5281/zenodo.1402449.
[64] B. Amélie and F. P. F.J., *Berger POPC/DOPE (50:50 ratio) MD simulation (300 K - 300ns - 1 bar)* (2018), URL https://doi.org/10.5281/zenodo.1402441.
[65] B. Amélie and F. P. F.J., *Berger pure DOPC MD simulation (300 K - 300ns - 1 bar)* (2018), URL https://doi.org/10.5281/zenodo.1402411.
[66] B. Amélie and F. P. F.J., *Berger DOPC/DOPE (50:50 ratio) MD simulation (300 K - 300ns - 1 bar)* (2018), URL https://doi.org/10.5281/zenodo.1402437.
[67] J. L. Browning and J. Seelig, Biochemistry **19**, 1262 (1980).
[68] F. Borle and J. Seelig, Chemistry and Physics of Lipids **36**, 263 (1985).
[69] J. Seelig and H. U. Gally, Biochemistry **15**, 5199 (1976).
[70] P. Mukhopadhyay, L. Monticelli, and D. P. Tieleman, Biophysical Journal **86**, 1601 (2004).
[71] W. Zhao, T. Róg, A. A. Gurtovenko, I. Vattulainen, and M. Karttunen, Biochimie **90**, 930 (2008), ISSN 0300-9084, URL http://www.sciencedirect.com/science/article/pii/S0300908408000692.
[72] J. Hénin, W. Shinoda, and M. L. Klein, The Journal of Physical Chemistry B **113**, 6958 (2009).
[73] M. Dahlberg, A. Marini, B. Mennucci, and A. Maliniak, The Journal of Physical Chemistry A **114**, 4375 (2010).
[74] P. M. Macdonald and J. Seelig, Biochemistry **26**, 1231 (1987).
[75] O. S. Ollila and G. Pabst, Biochimica et Biophysica Acta (BBA) - Biomembranes **1858**, 2512 (2016).
[76] J. Seelig, P. M. MacDonald, and P. G. Scherer, Biochemistry **26**, 7535 (1987).
[77] H. S. Antila, P. Buslaev, F. Favela-Rosales, T. Mendes Ferreira, I. Gushchin, M. Javanainen, B. Kav, J. J. Madsen, J. Melcr, M. S. Miettinen, et al., The Journal of Physical Chemistry B **0**, null (0), https://doi.org/10.1021/acs.jpcb.9b06091, URL https://doi.org/10.1021/acs.jpcb.9b06091.
[78] C. Paré and M. Lafleur, Biophysical Journal **74**, 899 (1998), ISSN 0006-3495, URL http://www.sciencedirect.com/science/article/pii/S0006349598740135.
[79] J. Pan, F. A. Heberle, S. Tristram-Nagle, M. Szymanski, M. Koepfinger, J. Katsaras, and N. Kučerka, Biochimica et Biophysica Acta (BBA) - Biomembranes **1818**, 2135 (2012).
[80] J. Melcr, H. Martinez-Seara, R. Nencini, J. Kolafa, P. Jungwirth, and O. H. S. Ollila, The Journal of Physical Chemistry B **122**, 4546 (2018).
[81] M. Roux and M. Bloom, Biochemistry **29**, 7077 (1990).
[82] H. Akutsu and J. Seelig, Biochemistry **20**, 7366 (1981).

ToDo